Title

Use of a Dual-Structure Constitutive Model for Predicting the Long-Term Behavior of an Expansive Clay Buffer in a Nuclear Waste Repository

Journal
International Journal of Geomechanics, 16(6)

ISSN
1532-3641

Authors
Vilarrasa, Víctor
Rutqvist, Jonny
Martin, Laura Blanco
et al.

Publication Date
2016-12-01

DOI
10.1061/(asce)gm.1943-5622.0000603

Peer reviewed

Use of a dual structure constitutive model for predicting the long-term behavior of an expansive clay buffer in a nuclear waste repository

Víctor Vilarrasa[1], Jonny Rutqvist[1], Laura Blanco Martin[1] and Jens Birkholzer[1]

[1] Lawrence Berkeley National Laboratory (LBNL), 1 Cyclotron Rd, Berkeley, CA 94720, USA

Version Accepted for Publication in

ASCE's International Journal of Geomechanics

https://doi.org/10.1061/(ASCE)GM.1943-5622.0000603

Final version published as:

Vilarrasa V., Rutqvist J., Blanco-Martin L., and Birkholzer J. Use of a dual structure constitutive model for predicting the long-term behavior of an expansive clay buffer in a nuclear waste repository. ASCE's International Journal of Geomechanics, 16, article number D4015005 (2016).

ABSTRACT

Expansive soils are suitable as backfill and buffer materials in engineered barrier systems to isolate high-level nuclear waste in deep geological formations. The canisters containing nuclear waste would be placed in tunnels excavated at several hundred meters depth. The expansive soil would be used for tunnel backfill and should provide enough swelling capacity to support the tunnel walls and thereby reduce the impact of the excavation damaged zone on permeability in the near-field that could affect the long-term barrier performance. In addition to their swelling capacity, expansive soils are characterized by accumulating irreversible strain upon suction cycles and by effects of microstructural swelling on water permeability that for backfill or buffer materials can significantly delay the time to reach full saturation. To simulate these characteristics of expansive soils, a dual structure constitutive model that includes two porosity levels is necessary. We present the formulation of the dual structure model and describe its implementation into a coupled fluid flow and geomechanical numerical simulator. We use the Barcelona Basic Model (BBM), which is an elasto-plastic constitutive model for unsaturated soils, to model the macrostructure, and we assume that the strains of the microstructure, which are volumetric and elastic, induce plastic strain to the macrostructure. We test and demonstrate the capabilities of the implemented dual structure model by modeling and reproducing observed behavior in two laboratory tests of expansive clay. As observed in the experiments, the simulations yield non-reversible strain accumulation upon suction cycles and a decreasing swelling capacity with increasing confining stress. Finally, we model, for the first time using a dual structure model, the long-term (100,000 years) performance of a generic high-level nuclear waste repository with waste emplacement in horizontal tunnels backfilled with expansive clay and hosted in a clay rock formation. We compare the thermo-hydro-mechanical results of the

dual structure model with those of the standard single structure BBM. The main difference between the simulation results using the two models is that the dual structure model predicts a time to fully saturate the expansive clay barrier in the order of thousands of years, while the standard single structure BBM yields a time in the order of tens of years. The saturation evolution of the buffer predicted by the dual structure model follows the short-term (up to 10 years) tendency observed in the mock-up test for the FEBEX in situ test, which gives confidence of the performance of the model. These examples show that a dual structure model, like the one presented here, is necessary to properly model the thermo-hydro-mechanical behavior of expansive soils.

Keywords: expansive soil; engineered barrier systems; unsaturated porous media; swelling; thermo-hydro-mechanical coupling.

1. INTRODUCTION

Expansive soils, among other applications, are suitable as backfill and buffer materials in engineered barrier systems (EBS) to isolate high-level nuclear waste in deep geological formations. The canisters containing nuclear waste would be placed in tunnels excavated at several hundred meters depth. Potential host rocks include granite (Gens et al., 2009, Dupray et al., 2013) and clay/shale formations (Gens et al., 2007; Rutqvist et al., 2014). The excavation of the tunnels will damage the surrounding rock, creating an excavation damaged zone (EDZ). The permeability in the EDZ may increase a few orders of magnitude (Tsang et al., 2005; Blümling et al., 2007; Alonso and Hoffmann, 2007), especially in the direction of the tunnel axis (Vilarrasa et al., 2011). This higher transport potential within the EDZ can be minimized by backfilling the tunnels with an unsaturated expansive soil, which will swell when hydrated by the host rock. Not only can the expansive soil backfill provide enough sustaining pressure to the tunnel wall to avoid collapse (Rutqvist et al., 2011), but can also provide enough swelling capacity so that the EDZ can be sealed, i.e., a reduction of hydraulic properties, especially in clay host rocks (Komine and Ogata, 1994; Tsang et al., 2005; Yu et al., 2014). However, healing, which implies not only a decrease in permeability, but also the recovery of the initial mechanical properties, is not observed in laboratory and field experiments (Yu et al., 2014).

Some field experiments, such as the full-scale engineered barriers experiment (FEBEX) (Alonso et al., 2005; Martinez-Landa and Carrera, 2005; Gens et al., 2009; Dupray et al., 2013), the HE-D in situ heating test (Gens et al., 2007) and the engineered barrier (EB) experiment (Alonso and Hoffmann, 2007), have been carried out to gain insight into the thermo-hydro-mechanical (THM) processes that occur during the heating and hydration of the EBS. The FEBEX experiment was performed at the Grimsel test site (Switzerland), in granite, and the HE-D and EB experiments at the Mont Terri site (Switzerland), in Opalinus clay. Though some analytical solutions, which can be very useful for probabilistic risk analysis (Tartakovsky, 2007; Jurado et al., 2012), have been developed to explain the processes occurring during heating/cooling and drying/hydration of the EBS (Chen and Ledesma, 2007), most of the studies use numerical models to reproduce the experiments and make long-term predictions (e.g. Gens et al., 2007; 2009; Rutqvist et al., 2008; 2014).

Some constitutive models exist to model non-isothermal unsaturated soils (Gens, 2010), such as the thermo-plasticity model proposed by Laloui and Cekerevac (2003) or the Barcelona Basic Model (BBM) (Alonso et al., 1990). The expansive soils forming the EBS, such as bentonite or a mixture of sand and expansive clay, have been extensively modeled adopting the BBM (e.g. Gens et al., 2007; 2009; Åkesson and Kristensson, 2008; Kristensson and Åkesson, 2008; Rutqvist et al., 2011; 2014). Though the BBM is a very appropriate constitutive model for unsaturated soils because it can reproduce important features of their behavior, like collapse when wetting occurs at a relatively high pre-consolidation stress, it cannot model certain aspects of expansive soils. These aspects include accumulation of irreversible strain upon suction cycles (Day, 1994; Al-Homoud et al., 1995; Tripathy et al., 2002) or effects of microstructural swelling on water permeability. The effect of microstructural swelling on water permeability has been observed to have a significant effect on resaturation of expansive soil barriers, for example at the mock-up test performed at CIEMAT, Madrid (Spain), which reproduces a large-scale heating test of a bentonite buffer (Sánchez et al., 2012).

To rigorously model these characteristics of expansive soils, it is necessary to use a dual structure constitutive model that acknowledges the existence of two porosity levels (Gens and Alonso, 1992; Alonso et al., 1999; Gens et al., 2006; Sánchez et al., 2005; 2008). Expansive clays present a bimodal or trimodal pore size distribution (Figure 1) in which the pores having a diameter smaller than 0.1 μm correspond to voids inside clay aggregates and the larger pores correspond to pores between clay aggregates (Dixon et al., 1999; Villar, 1999; Delage et al., 2006; Wang et al., 2013b). This leads to the differentiation of a microstructure, which is made of the active clay minerals, and a macrostructure, which is formed by the global distribution of clay aggregates and the macropores between them (Figure 2).

Fluids can flow solely through the macroporosity (Wang et al., 2013a). As the liquid saturation degree of the clay increases (suction decreases), water layers are inserted between the microstructure clay layers and thus swelling occurs because the volume of clay particles increases (Saiyouri et al., 2000). This causes the microporosity to invade the macroporosity as the expansive soil hydrates, which may reduce its permeability by several orders of magnitude (Olivella and Gens, 2000; Alonso and Hoffmann, 2007). This permeability reduction as the liquid saturation degree increases can explain delays in the saturation time that have been observed at both mock-up and in situ experiments involving expansive soil barriers (Sánchez et al., 2012). Therefore, the use of a dual structure constitutive model is required to properly simulate the THM behavior of expansive soils used as buffer material to backfill the space between the canisters containing nuclear waste and the tunnel walls.

The aims of this paper are to present the dual structure model that has been implemented in the TOUGH-FLAC simulator (Rutqvist et al., 2011) and to analyze the differences in the long-term performance of a generic nuclear waste repository in a clay host rock when modeling the expansive soil backfill either with the standard single structure BBM or the dual structure model. To do so, we first present the mathematical formulation of the dual structure model. Then, we show the capabilities of the model by reproducing a laboratory test in which irreversible expansion accumulates upon suction cycles. Finally, we model the long-term THM response of a generic repository for geological disposal of high-level nuclear waste adopting either the standard single structure BBM or the dual structure model as a constitutive model for the expansive soil. Such long-term simulation, of 100,000 years, is novel and will permit shedding light on the long-term performance of the expansive clay that constitutes the buffer using the dual structure constitutive model.

2. DUAL STRUCTURE MODEL IMPLEMENTATION IN TOUGH-FLAC

In this section, the development and implementation of a dual structure model for expansive soils into TOUGH-FLAC is presented. First, an overview of the basic equations in the dual structure model following (in part) the developments by Alonso et al. (1999) and Sánchez et al. (2005) is presented. Finally, the implementation of this model into TOUGH-FLAC is summarized.

2.1. The dual structure approach

The dual structure model considers the existence of a macrostructure, a microstructure and the interactions between them. The macrostructure can be modeled with a constitutive model for unsaturated soils, such as the BBM. The BBM is able to describe many typical features of the mechanical behavior of unsaturated soils, including wetting-induced swelling or collapse strains (depending on the magnitude of the applied stress), as well as the increase in shear strength and apparent pre-consolidation stress with suction (Gens et al., 2006). The extension of BBM to a dual structure model enables simulating the behavior of expansive soils, such as the dependency of swelling strains and swelling pressures on the initial stress state and on the stress path, strain accumulation upon suction cycles and secondary swelling. It is believed that such behavioral features are mainly related to the existence of coupled chemical-hydrogeological-mechanical phenomena between distinct levels of structure within the material (Alonso et al., 1999).

Conceptually, in a dual structure model, as described by Alonso et al. (1999) and Sánchez et al. (2005), the total volume, V, of the material consists of the solid phase, V_s, the microstructural voids V_{vm}, and the macrostructure voids V_{vM}

$$V = V_s + V_{vm} + V_{vM} = V_m + V_{vM} \quad , \tag{1}$$

where V_m is the volume of the microstructure.

Additionally, the total void ratio, e, and porosity, φ, are the sum of their microstructural and macrostructural components according to

$$e = \frac{V_v}{V_s} = \frac{V_{vM}}{V_s} + \frac{V_{vm}}{V_s} = e_M + e_m, \qquad (2)$$

$$\varphi = \frac{V_v}{V} = \frac{V_{vM}}{V} + \frac{V_{vm}}{V} = \varphi_M + \varphi_m, \qquad (3)$$

where V_v is the total volume of voids and the subscripts m and M refer to the microstructure and the macrostructure, respectively.

The microstructure can swell to invade the macroporosity, depending on the mechanical confinement and load level. This is relevant when considering permeability changes during the expansive soil swelling, because fluid flow takes place through the macroporosity, which is not proportional to the total strain and deformation of the expansive soil.

2.2. Macrostructural level

The macrostructural behavior is modeled based on the BBM, in which the yield surface is defined in the $p - q - s$ space, where p is net mean stress (i.e., total stress minus gas-phase pressure), q is deviatoric stress (or shear stress), and s is suction (i.e., gas pressure minus liquid pressure). The size of the elastic domain increases as suction increases. This is shown in Figure 3 in the isotropic stress (*s*-*p* space) plane. The rate of the increase of the elastic domain, represented by the loading-collapse (LC) curve, is one of the fundamental characteristics of the BBM (Gens et al., 2006).

The suction-dependent loading-collapse (LC) yield surface bounds the elastic region according to

$$f_{LC} = \frac{q^2}{g_y(\theta)^2} - \frac{M^2}{g_y(\theta=0)^2}(p+p_s)(p_0-p) = 0 \tag{4}$$

where θ is the Lode angle, the function $g_y(\theta)$ describes the shape of the yield surface in the deviatoric plane, M is the constant slope of the critical state line, $p_s = k_s s$ represents the increase in cohesion with suction, k_s is an empirical material constant and function

$$p_0 = p^c \left(\frac{p_0^*}{p^c}\right)^{[\lambda_{Ps0} - \kappa_{Ps0}]/[\lambda_{Ps} - \kappa_{Ps0}]} \tag{5}$$

is the net mean yield stress (or apparent pre-consolidation stress) at current suction, where p_0^* is the net mean yield stress (or pre-consolidation stress) at full saturation, p^c is a reference stress, λ_{Ps0} is a compressibility parameter in virgin soil states at zero suction,

$\lambda_{Ps} = \lambda_{Ps0}\left[(1-r)\exp(-\xi s) + r\right]$ is a compressibility parameter in virgin soil states at suction s, r is a constant related to the maximum stiffness of the soil (for an infinite suction), ξ is a parameter that controls the rate of increase of soil stiffness with suction and κ_{Ps0} is the elastic stiffness parameter for changes in net mean stress at zero suction.

The flow rule is given by

$$g_{LC} = \frac{\alpha_a q^2}{g_y(\theta)^2} - \frac{M^2}{g_y(\theta=0)^2}(p+p_s)(p_0-p) \qquad (6)$$

where α_a is a parameter that gives rise to a non-associative model, i.e., $g_{LC} \neq f_{LC}$.

2.3. Microstructural level

The following assumptions are adopted related to microstructural behavior and its interaction with the macrostructure:

- The microstructure is mainly saturated and the effective stress concept holds
- The microstructural behavior is elastic and volumetric
- Mechanical, hydraulic, and chemical equilibrium exists between microstructure and macrostructure
- Coupling between microstructure and macrostructure results in a possible buildup of macrostructural elastoplastic strains when elastic microstructural strains occur

With these assumptions, the volumetric microstructural strain, $\mathrm{d}\varepsilon_{vm}^{e}$, depends exclusively on variations of mean effective stress,

$$\mathrm{d}\hat{p} = \mathrm{d}\left(\bar{p} - p_l\right) = \mathrm{d}\left(\bar{p} - p_g + p_g - p_l\right) = \mathrm{d}\left(p + s\right), \tag{7}$$

where $\bar{p}$ is mean stress, p_l is liquid phase pressure and p_g is gas phase pressure. Therefore, a straight line $p + s = constant$ can be drawn in the *p*-*s* space around the current state of stress and suction along which no microstructural strain takes place (Figure 3). This line, called the Neutral Line (NL), moves with the current stress state (C) and separates at each instant the zone of microstructural swelling from the zone of microstructural shrinkage in the $p - s$ plane (Figure 3).

2.4. Interaction between structural levels

Microstructural swelling/shrinkage affects the structural arrangement of the macrostructure, inducing irreversible strains in the macroporosity. These irreversible macrostructural deformations induced by microstructural effects are considered proportional to the microstructural strain through interaction functions as

$$\mathrm{d}\varepsilon_{v\beta}^{p} = f\mathrm{d}\varepsilon_{vm}^{e} \tag{8}$$

where $\varepsilon_{v\beta}^{p}$ is the macrostructural plastic strain arising from the interaction between both structures. Two interaction functions are defined: $f = f_c$ for microstructural compression or shrinkage paths and $f = f_s$ for microstructural swelling paths. These functions can adopt several forms (Sánchez et al., 2005), but they always depend on the ratio p/p_0

$$f_c = f_{c0} + f_{c1}(p/p_0)^{n_c} \quad \text{and} \quad f_s = f_{s0} + f_{s1}(1 - p/p_0)^{n_s}, \tag{9a}$$

or

$$f_c = f_{c0} + f_{c1}\tanh\left[f_{c2}(p/p_0 - f_{c3})\right] \quad \text{and} \quad f_s = f_{s0} - f_{s1}\tanh\left[f_{s2}(p/p_0 - f_{s3})\right], \tag{9b}$$

where f_{ij} and n_i ($i = \{c, s\}$ and $j = \{0,1,2,3\}$) are constants.

The ratio p/p_0 is a measure of the distance from the current stress state to the yield locus for the macrostructure LC and has the same meaning as the overconsolidation ratio for an isotropically consolidated soil. A low p/p_0 implies a dense packing of the material. Under such dense packing (dense macrostructure), the microstructural swelling strongly affects the global arrangement of clay aggregates, which becomes more open. This results in a softening of the macrostructure, which implies that the macrostructural yield surface LC shrinks. Under this condition, expansion accumulates upon suction cycles. On the other hand, a high p/p_0 implies a looser macrostructure. Under such loose packing conditions, the microstructural swelling produces an invasion of the macropores, which tends to close the macrostructure and compression accumulates upon suction cycles. In such a case, the elastic domain increases and LC expands (Alonso et al. 1999; Sánchez et al., 2005).

2.5. Elastic Strain

Equivalently to the BBM model, the macrostructural volumetric elastic strain increment for the dual structure model is associated with changes in net mean stress $\mathrm{d}p$ and suction $\mathrm{d}s$ (Alonso et al., 1999)

$$\mathrm{d}\varepsilon_{vM}^{e} = \frac{1}{K_M}\mathrm{d}p + \frac{1}{K_s}\mathrm{d}s, \qquad (10)$$

where K_M is the macrostructural bulk modulus and K_s is the macrostructural modulus associated with suction strain. K_M and K_s are defined as

$$K_M = \frac{(1+e_M)p}{\kappa_{Ps}(s)}, \qquad (11)$$

$$K_s = \frac{(1+e_M)(s+p_{atm})}{\kappa_{sp}(p,s)} \qquad (12)$$

where $\kappa_{Ps} = \kappa_{Ps0}(1 + s\alpha_{ps})$, $\kappa_{sp} = \kappa_{sp0}(1 + \alpha_{sp}\ln(p/p_{ref}))\exp(\alpha_{ss}s)$ and κ_{Ps0} and κ_{sp0} are compressibility parameters for changes in net mean stress and suction, respectively. p_{ref} is a reference stress state for relating elastic compressibility to suction and α_{ps}, α_{sp} and α_{ss} are empirical parameters.

The microstructural volumetric strain depends on the change in the microstructural effective stress

$$\mathrm{d}\varepsilon_{vm}^{e} = \frac{1}{K_m}\mathrm{d}\hat{p}, \tag{13}$$

where K_m is the microstructural bulk modulus for changes in mean effective stress. Alonso et al. (1999) define two alternative expressions for the microstructural modulus

$$K_m = \frac{(1+e_m)\hat{p}}{\kappa_m}, \tag{14a}$$

$$K_m = \frac{e^{\alpha_m \hat{p}}}{\beta_m}, \tag{14b}$$

where κ_m, α_m and β_m are compressibility parameters.

Thermal strains are purely volumetric

$$\mathrm{d}\varepsilon_v^T = (\alpha_0 + 2\alpha_2 \Delta T)\mathrm{d}T, \tag{15}$$

where α_0 and α_2 are material parameters corresponding to a temperature-dependent volumetric thermal expansion coefficient and T is temperature.

The deviatoric elastic strain increment of the macrostructure is defined as

$$\mathrm{d}e_{qM}^{e} = \frac{1}{3G}\mathrm{d}q, \tag{16}$$

where G is the shear modulus and may be obtained using a constant Poisson ratio ν in

$$G = \frac{3(1-2\nu)}{2(1+\nu)} K_M. \tag{17}$$

Thus, the equations for elastic mechanical strain indicate the dependency of bulk modulus on suction (and hence fluid saturation), which in a dry clay can be significantly stiffer than in a water-saturated clay.

In total, the BBM is characterized by 18 parameters and the dual structure model incorporates between 8 and 11 additional parameters, depending on the microstructural bulk modulus and the interaction functions that are used.

2.6. Plastic Strain

Macrostructural plastic strain occurs by two possible mechanisms: either when the stress lies on the LC yield surface, or as a result of microstructural shrinkage/swelling. While the plastic strain by microstructural shrinkage/swelling is described by Eq. (8), the LC plastic strains are obtained from the plastic flow rule

$$\mathrm{d}\varepsilon_{vLC}^{p} = \mathrm{d}\Lambda \frac{\partial g_{LC}}{\partial p}, \tag{18}$$

$$\mathrm{d}\varepsilon_{qLC}^{p} = \mathrm{d}\Lambda \frac{\partial g_{LC}}{\partial q}, \tag{19}$$

where $\mathrm{d}\Lambda$ is the plastic multiplier obtained from the consistency condition $\mathrm{d}f_{LC} = 0$ (recall Eq. (4)). The calculation of the plastic multiplier $\mathrm{d}\Lambda$ is detailed in Rutqvist et al. (2011).

The total plastic volumetric strain is the sum of both plastic mechanisms

$$\mathrm{d}\varepsilon_{v}^{p} = \mathrm{d}\varepsilon_{vLC}^{p} + \mathrm{d}\varepsilon_{v\beta}^{p}. \tag{20}$$

The hardening variable of the macrostructure — the pre-consolidation pressure p_0^* —depends on the total plastic volumetric strain $\mathrm{d}\varepsilon_v^p$ as

$$\frac{\mathrm{d}p_0^*}{p_0^*} = \frac{(1+e_M)\mathrm{d}\varepsilon_v^p}{\lambda_{Ps0} - \kappa_{Ps0}}. \tag{21}$$

2.7. *Implementation into TOUGH-FLAC*

We implemented the dual structure model in TOUGH-FLAC, by extending the previous implementation of the BBM (Rutqvist et al., 2011) to include the microstructural level and its interactions with the macrostructure. This involves consideration of the sequential coupling of the TOUGH2 and FLAC^{3D} simulators (Rutqvist, 2011), and constitutive stress-strain behavior in FLAC^{3D}. TOUGH2 is a multi-phase non-isothermal finite volume code. FLAC^{3D} is a geomechanics finite difference code. This implementation of the dual structure model in FLAC^{3D} was done using the User Defined constitutive Model (UDM) option in FLAC^{3D}, including C++ coding and dynamic link libraries. Specifically, the following calculation items were added

1) Microstructural strain (Eq. 13) and effective stress (Eq. 7)

2) Macrostructural strain (Eq. 10)

3) Global elastic tensor depending on microscopic and macroscopic structural compliances (Sanchez et al., 2005)

4) Micro/macrostructural interaction functions (Eqs. 9a and 9b)

5) Plastic macrostructural strain from structural interactions (Eq. 8)

6) Plastic corrections in the FLAC^{3D} elastoplastic algorithm (Eqs. 18, 19 and 20)

7) Plastic hardening/softening factors (Eq. 21)

Finally, at the end of each FLAC^{3D} step, the hardening parameter, i.e., the pre-consolidation pressure p_0^*, the bulk modulus of both microstructure and macrostructure and the tangential bulk modulus, are updated based on the total plastic volumetric strain and stress state, and these are stored for use in the next step.

3. MODEL CAPABILITIES

We test and demonstrate the capabilities of the dual structure model implemented in TOUGH-FLAC by modeling a laboratory experiment of Pousada (1982), in which an expansive clay undergoes several suction (wetting-drying) cycles for two net mean stresses (Figures 4 and 5). Expansive clays show a non-reversible behavior when they undergo successive wetting-drying cycles. This phenomenon cannot be reproduced with the standard single structure BBM model, but the incorporation of the interactions between the microstructure and the macrostructure of an expansive soil allows accumulating plastic strain upon suction cycles. Table 1 shows the parameters of the dual structure model resulting from the calibration of the laboratory experiments of Pousada (1982).

Figure 4 shows the calibration of a suction cycles test, which comprises 5 suction cycles (suction ranges from 1.7 to 0.2 MPa in each suction cycle) at a very low net mean stress (0.01 MPa). The model can reproduce the plastic strain accumulation upon cycles and the tendency to reduce the amount of plastic strain accumulated between two successive suction cycles as cycles accumulate. The calibration of the experiment reproduces with a fair accuracy the end points of the wetting-drying cycles as well as the strain evolution of the first suction cycle, which is curved. Nevertheless, the strain evolution of the subsequent cycles becomes quite linear in the laboratory experiment, but the numerical results maintain the curved evolution. To improve this change in the strain evolution pattern as suction cycles evolve, a more complex bulk modulus of both the microstructure and macrostructure may need to be proposed.

While the microstructure behaves elastically (Figure 4b), the macrostructure undergoes plastic strain that causes irreversible changes in macroporosity, which is related to the macrostructural void ratio through $\varphi_M = e_M/(1+e)$ (Figure 4c). Macroporosity is enhanced at low net mean stress (low values of the p/p_0 ratio) as a result of the interaction between the two levels of structures.

Low values of the p/p_0 ratio imply a dense macrostructure, so the swelling of the microstructure will open up the macrostructure, inducing expansion upon suction cycles. Thus, the plastic strain of the macrostructure induced by the elastic volumetric strain of the microstructure is higher during wetting than during drying (Figure 4d).

Figure 5 displays the results of the same experiment, but performed at a higher net mean stress of 0.1 MPa. Similarly to the experiment with a lower confining pressure, the numerical calibration reproduces fairly well the end points of the wetting-drying cycles and the curved strain evolution of the first cycle. But for subsequent suction cycles, the experimental strain evolution becomes quasi-linear, while the numerical simulation keeps the curved evolution. Comparison between Figures 4 and 5 reveals that the swelling capacity of the material is reduced as the confining stress increases. The rest of the characteristics remain the same: the microstructure is elastic, plastic strain accumulation is reduced with the number of cycles and expansion accumulates upon cycles. The latter occurs because the p/p_0 ratio is still relatively low and therefore, the macrostructure is dense.

For a net mean stress that would yield a high p/p_0 ratio, the macrostructure would be loose and micropores would invade macropores upon suction cycles. In this case, given the net mean stress and suction values, the microstructure deformation is almost independent of the confining stress (recall Figures 4b and 5b) because its stiffness is proportional to the effective stress (Eq. (14)), which evolves very similarly in the two experiments. Apart from this, the higher net mean stress in the experiment performed under 0.1 MPa implies a higher p/p_0 ratio and therefore, the suction cycles are closer to the equilibrium point between the wetting and the drying interaction functions. This causes a smaller plastic strain accumulation upon suction cycles due to the interaction between the two structural levels (recall Figures 4d and 5d).

The calibration of the dual structure model with only these two available experiments becomes quite complicated due to the large number of degrees of freedom that this model has. Though the simulated deformation paths differ somewhat from the experimental results, the global behavior of this expansive clay is satisfactorily captured. In general, more experiments would be required to adjust most of the parameters of the dual structure model. Actually, this will be needed to model bentonite buffers that are intended for use in high-level nuclear waste repositories.

4. APPLICATION TO A GENERIC REPOSITORY

We apply the dual structure model and compare the THM results with those of the standard single structure BBM in a generic repository similar to that considered in the Swiss nuclear waste disposal program. The long-term (100,000 years) behavior of such repository is simulated. The host rock is assumed to be Opalinus clay. The tunnels containing the high-level waste are placed at 500 m deep and are spaced 50 m. Since the emplacement tunnels may typically be up to 1 km long, we model a 2D cross section of the repository and make use of the symmetry to model only one tunnel. We further assume that the tunnel is backfilled with FEBEX bentonite (Gens et al., 2009; Sanchez et al., 2012). Thus, the dual structure properties of the backfill are different than those calibrated from the experimental results presented in Section 3. The geometry of the model and the heat load of the waste are displayed in Figure 6 (Rutqvist et al., 2014).

Table 2 compiles the material parameters of the claystone host rock. The properties of the Opalinus clay are taken from Gens et al. (2007) and Corkum and Martin (2007). The relative permeability curves follow the van Genuchten-Mualem model. The properties of the FEBEX bentonite for the standard single structure BBM model were derived by Alonso et al. (2005) and Gens et al. (2009) (Table 3) and were also used in Rutqvist et al. (2014). The properties for the macrostructure of the dual structure model are similar to those used in the single structure BBM model, but some parameters have been adapted to obtain a global behavior of both the microstructure and the macrostructure comparable to that of the BBM model (see Table 4). The properties of the microstructure of the dual structure model for the FEBEX bentonite are based on those proposed by Sanchez et al. (2012), but with some modifications (Table 4).

We assume that the intrinsic permeability varies according to an exponential law that was proposed and calibrated against laboratory measurements by Sanchez et al. (2012) for the dual structure model. This law depends on the porosity of the macrostructure as

$$\mathbf{k} = k_0 \exp\left[b\left(\varphi_M - \varphi_{M0}\right)\right]\mathbf{I}, \tag{22}$$

where $\mathbf{k}$ is the intrinsic permeability tensor, k_0 is the intrinsic permeability at the reference porosity of the macrostructure φ_{M0}, b is a model parameter and $\mathbf{I}$ is the identity matrix. For the single structure BBM model, the same law is adopted, but changing macroporosity by total porosity and adjusting the value of k_0, so that the initial permeability is the same in the two cases ($2.0\mathrm{x}10^{-21}$ m^2). Furthermore, to account for the higher intrinsic permeability of clays to gas than to water (Olivella and Gens, 2000), we make use of the relationship given by Klinkenberg (1941)

$$\mathbf{k}_{gas} = \mathbf{k}\left(1 + \frac{b_k}{p_g}\right), \tag{23}$$

where b_k is the Klinkenberg parameter.

To calculate consistent initial conditions of the repository once the emplacement tunnel has been excavated and the backfill and the waste placed inside the tunnel, a sequence of stages is calculated. First, we calculate the pre-excavation equilibrium conditions. Mechanically, the stress field is assumed isotropic and the vertical total stress increases linearly with depth and proportionally to a bulk density of 24 kN/m^3. Since the tunnel is located at 500 m depth, the pre-excavation mean stress is 11.8 MPa. The mechanical boundary conditions are no displacement perpendicular to the lateral and bottom boundaries and a constant pressure equal to atmospheric pressure at the upper boundary. Hydraulically, the groundwater table is located at the ground surface. Fluid pressure is imposed at the bottom of the model, at 1000 m depth, and is set to 9 MPa. The ground surface temperature and the temperature at the bottom of the model are fixed to 10 ºC and 40 ºC, respectively. Thus, the geothermal gradient is equal to 30 ºC/km. Next, the drift excavation is simulated by removing the elements in the tunnel and fixing the temperature to 25 ºC and the fluid pressure to 0.1 MPa until steady state is reached. Finally, the nuclear waste canister and the bentonite buffer are placed in the tunnel instantaneously and the waste starts to release heat. The bentonite has an initial liquid degree of saturation of 0.65 and the gas pressure is initially fixed at 0.1 MPa.

Figure 7 shows the evolution of temperature, liquid saturation degree, fluid pressure and total mean stress at some points within the buffer and in the Opalinus clay obtained with both the BBM and the dual structure model. Temperature evolution is similar for both mechanical constitutive models, though the temperature peak is slightly higher close to the canister for the dual structure model because the buffer becomes drier than for the standard single structure BBM (Figure 7a). However, the hydration of the buffer is significantly affected by the mechanical constitutive model (Figure 7b). While the buffer close to the canister becomes fully saturated after 60 years for the BBM, it takes up to 2780 years when using the dual structure model. This is the first time that the time for full saturation of the buffer has been predicted, because previous simulations did not go beyond some tens of years (recall that we simulated 100,000 years). Though the exact time at which the buffer will become fully saturated is very uncertain because we do not know with precision all the parameters of the dual structure model, the difference of two orders of magnitude between the saturation time predicted by the BBM and the dual structure model shows the importance of using a constitutive model that accounts for two structural levels to reproduce the thermo-hydro-mechanical behavior of expansive clays.

This difference in the saturation time of the buffer occurs because in the dual structure model the porosity through which fluids flow is only the porosity of the macrostructure and not the total porosity, like in the BBM. The deviation in the saturation evolution in the inner part of the buffer between the two models starts at early times (2-3 years), which is in agreement with the observations of the 10 year-long mock-up test for the FEBEX in situ test performed at the laboratory at CIEMAT, Madrid (Spain) (see Sanchez et al., 2012 for details). Furthermore, the delay in the saturation of the bentonite buffer causes a delay in its pressurization close to the canister (Figure 7c). Figure 7c displays that, close to the canister, the increase in fluid pressure, which equals the maximum pressure of the fluids filling the pores, i.e., gas pressure if the soil is unsaturated and liquid pressure if the soil is saturated, is significantly delayed. But once the buffer is fully saturated, the thermal pressurization is similar to that of the buffer close to the tunnel wall. Despite this significant delay in saturation at the inner parts of the buffer, the overall buffer swelling stress evolution is not severely retarded (Figure 7d). Indeed, the buffer is still functioning to provide sufficient swelling and support load to the tunnel wall and the EDZ (Figure 8). The swelling stress of a few MPa has the potential to close the fractures of the EDZ, significantly reducing permeability of the EDZ and assuring sealing in the long-term.

Figure 9 displays the variables that control the dual structure constitutive model, i.e., suction, mean net stress and effective stress. While suction and mean net stress are used to calculate the behavior of the macrostructure according to the BBM, the mean effective stress determines the elastic volumetric strain of the microstructure in the dual structure model. Suction close to the tunnel wall decreases from the beginning of the simulation because the host rock, which is fully saturated, supplies groundwater that gradually saturates the bentonite buffer (Figure 9a). However, suction increases initially close to the canister because the heat of the high-level nuclear waste dries the bentonite. Subsequently, the saturation of the whole bentonite buffer starts to take place and suction decreases. The net mean stress (Figure 9b) is similar for both models close to the tunnel wall because of the relatively quick saturation of this part of the buffer, which leads to a comparable high stiffness of the expansive clay (Figure 9d). However, close to the canister, the net mean stress becomes much higher for the dual structure model than for the BBM because the higher suction (recall Figure 9a) leads to a stiffer bentonite (Figure 9d).

The effective mean stress evolution (Figure 9c) is similar to the suction evolution because the net mean stress is relatively low.

Figure 10 illustrates porosity evolution for simulation results of both constitutive models. The total porosity changes, though larger in the dual structure model, are relatively similar for both models, especially in the region of the buffer close to the tunnel wall. However, a higher porosity reduction occurs close to the waste overpack, where a stronger drying takes place when accounting for the dual structure model. Interestingly, the reduction in macroporosity is larger than the reduction in total porosity close to the waste overpack. This larger macroporosity reduction in the dual structure model leads to a greater permeability reduction close to the waste overpack that impedes hydration of the buffer (Figure 11).

Figure 12 schematically illustrates the evolution of the microporosity and the macroporosity in a point close to the canister and in another point close to the tunnel wall. The expansive clay close to the tunnel wall becomes saturated at a low mean stress. Thus, both the microstructure and the macrostructure swell (strain is negative according to the sign criterion of geomechanics) and since the interaction function of swelling at low stress is positive (Figure 12b), the plastic strain of the macrostructure due to interaction between the two structural levels is negative, i.e., the macrostructure expands (Figure 12a). Therefore, the permeability of the clay increases and full saturation occurs relatively quickly.

On the other hand, close to the canister, the buffer dries during the first year of simulation, leading to shrinkage at low stress (strain is positive). In this case, since the interaction function of shrinkage at low stress is positive, the plastic strain of the macrostructure due to interaction between the two structural levels is positive, which implies shrinkage of the macrostructure and therefore, a permeability reduction. Later, the permeability is reduced even further because the mean stress of the buffer increases, which causes a compression of the pores. Finally, the region around the canister is saturated at high stress. Under these conditions, the microstructure swells (strain is negative), but the interaction function of swelling at high stress is negative (Figure 12b). As a result, the plastic strain of the macrostructure due to interaction between the two structural levels is positive, i.e., the macrostructure shrinks. This shrinkage of the macrostructure is caused by an invasion of the microstructure, which closes the macropores when the expansive clay swells at high stress, contributing to reduce the permeability. This greater permeability reduction around the waste overpack when using the dual structure model causes a significant delay in the time at which the buffer becomes fully saturated.

These results are in agreement with the short-term results of Sanchez et al. (2012), who modeled a large-scale heating test—a mock-up test for the FEBEX in situ test—performed at the laboratory that lasted for 10 years. Their modeling results reproduce the experimentally observed delay of the saturation of the buffer in the short-term when using the dual structure model instead of the BBM. Here, we show how such a delay might affect the long-term THM evolution of a repository. Future code comparison of the dual structure model will be valuable. The independent implementation of the dual-structure model into a different code, as conducted in this study, provides the possibilities of performing such code comparison and additional validations. This will lead to increased confidence in the long-term predictions of these complex and important processes.

5. CONCLUSIONS

The dual structure model accounts for two structural levels to model the THM behavior of an expansive soil, i.e., the microstructure and the macrostructure, and the interactions that occur between them. We have presented the formulation of the dual structure model and described its implementation into the coupled fluid flow and geomechanical simulator TOUGH-FLAC. Furthermore, we have shown the capabilities of the dual structure model by modeling and reproducing observed behavior for two laboratory tests performed by Pousada (1982) on expansive clay under increasing confining stress. In agreement with observations in the laboratory, the simulations yielded non-reversible strain accumulation upon suction cycles and a decreasing swelling capacity as the confining stress increases. Finally, we have modeled the long-term performance of a generic high-level nuclear waste repository with a bentonite back-filled waste emplacement tunnel and compared the results of both the dual structure model to that of a standard single structure model equivalent to the Barcelona Basic Model (BBM).

The main difference between the two models is that the dual structure model predicts that the time for full saturation of the expansive clay is of thousands of years, while the BBM yields a time of tens of years. The numerical simulation shows that this delay is caused by the fact that the fluid flow conducting macrostructure is invaded by the microstructure with associated reduction in permeability for water flow. Such a delay has previously been observed in large-scale laboratory and in situ experiments and here we show this might affect the long-term performance of a repository. This result shows evidence that to properly simulate the THM behavior of expansive soils, a dual structure model, like the one presented here, should be used. However, the modeling results also showed that despite a significant delay in saturation at the inner parts of the buffer, the overall buffer swelling stress evolution was not severely retarded.

That is, the buffer is still functioning to provide sufficient swelling and support load to the tunnel wall and the EDZ.

ACKNOWLEDGEMENTS

Funding for this work was provided by the Used Fuel Disposition Campaign, Office of Nuclear Energy, of the US Department of Energy under Contract Number DE-AC02-05CH11231 with Berkeley Lab.

REFERENCES

Al-Homoud, A.S., Basma, A.A., Malkawi, A.I.H., Al-Bashabsheh, M.A. Cyclic swelling behavior of clays. *J. Geotech. Engrg.*, **121**, 562–565 (1995).

Alonso, E.E., Gens, A., Josa, A. A constitutive model for partially saturated soils. *Geotechnique*, **40**, 405–430 (1990).

Alonso, E.E., Vaunat, J., Gens, A. Modelling the mechanical behaviour of expansive clays. *Engineering Geology*, **54**, 173–183 (1999).

Alonso, E.E., Alcoverro, J., Coste, F., Malinsky, L., Merrien-Soukatchoff, V., Kadiri, I., Nowak, T., Shao, H., Nguyen, T.S., Selvadurai, A.P.S., Armand, G., Sobolik, S.R., Itamura, M., Stone, C.M., Webb, S.W., Rejeb, A., Tijani, M., Maouche, Z., Kobayashi, A., Kurikami, H., Ito, A., Sugita, Y., Chijimatsu, M., Borgesson, L., Hernelind, J., Rutqvist, J., Tsang, C., Jussila, P. The FEBEX benchmark test: case definition and comparison of modeling approaches. *Int. J. Rock Mech. Min. Sci.*, **42**, 611–638 (2005).

Alonso, E.E., Hoffmann, C. Modelling the field behaviour of a granular expansive barrier. *Physics and Chemistry of the Earth*, **32**, 850–865 (2007).

Åkesson, M., Kristensson, O. Mechanical modeling of MX-80 – Development of constitutive laws. *Physics and Chemistry of the Earth*, **33**, S504–S507 (2008).

Blümling, P., Bernier, F., Lebon, P., Martin, C.D. The excavation damaged zone in clay formations time-dependent behaviour and influence on performance assessment. *Phys Chem Earth*, **32**, 588–599 (2007).

Chen, G.J., Ledesma, A. Coupled solution of heat and moisture flow in unsaturated clay barriers in a repository geometry. *Int. J. Numer. Anal. Meth. Geomech*., **31**, 1045–1065 (2007).

Corkum, A.G., Martin, C.D. The mechanical behaviour of weak mudstone (Opalinus Clay) at low stresses. *Int. J. Rock Mech. Min. Sci.*, **44**, 196–209.

Day, R.W. Swell-shrink behavior of compacted clay. *J. Geotech. Engrg.*, **120**, 618–623 (1994).

Delage, P., Marcial, D., Cui, Y.J., Ruiz, X. Ageing effects in a compacted bentonite: a microstructure approach. *Geotechnique,* **56**(5), 291–304 (2006).

Dixon, D.A., Graham, J., Gray, M.N. Hydraulic conductivity of clays in confined tests under low hydraulic gradients. *Can. Geotech. J.* **36**, 815–825 (1999).

Dupray, F., François, B., Laloui, L. Analysis of the FEBEX multi-barrier system including thermoplasticity of unsaturated bentonite. *Int. J. Numer. Anal. Meth. Geomech*., **37**, 399–422 (2013).

Gens, A, Alonso, E. A framework for the behaviour of unsaturated expansive clays. *Can. Geotech. J.* **29**, 1013–1032 (1992).

Gens, A., Sánchez, M., Sheng, D. On constitutive modelling of unsaturated soils. *Acta Geotechnica*, **1**, 137–147 (2006).

Gens, A., Vaunat, J., Garitte, B., Wileveau, Y. In situ behaviour of a stiff layered clay subject to thermal loading, observations and interpretation. *Geotechnique*, **57**(2), 207–228 (2007).

Gens, A., Sanchez, M., Guimaraes, L. do N., Alonso, E.E., Lloret, A., Olivella, S., Villar, M.V., Huertas, F. A full-scale in situ heating test for high-level nuclear waste disposal: observations, analysis and interpretation. *Geotechnique*, **59**(4), 377–399 (2009).

Gens, A. Soil - environmental interactions in geotechnical engineering. *Geotechnique*, **60**, 3–74 (2010).

Jurado, A., de Gaspari, F., Vilarrasa, V., Bolster, D., Sánchez-Vila, X., Fernández-García, D., Tartakovsky, D.M. Probabilistic analysis of groundwater-related risks at subsurface excavation sites. *Engineering Geology*, **125**, 35–44 (2012).

Klinkenberg, L.J. The Permeability of Porous Media to Liquids and Gases, in *API Drilling and Production Practice*, 200–213 (1941).

Komine, H., Ogata, N. Experimental study on swelling characteristics of compacted bentonite. *Can. Geotech. J.* **31**, 478–490 (1994).

Kristensson, O., Åkesson, M. Mechanical modeling of MX-80 – Quick tools for BBM parameter analysis. *Physics and Chemistry of the Earth*, **33**, S508–S515 (2008).

Laloui, L., Cekerevac, C. Thermo-plasticity of clays: An isotropic yield mechanism. *Computers and Geotechnics*, **30**, 649–660 (2003).

Lloret, A., Villar, M.V., Sanchez, M., Gens, A., Pintado, X., Alonso, E.E. Mechanical behaviour of heavily compacted bentonite under high suction changes. *Géotechnique*, **53**(1), 27-40 (2003).

Martinez-Landa, L., Carrera, J. An analysis of hydraulic conductivity scale effects in granite (Full-scale Engineered Barrier Experiment (FEBEX), Grimsel, Switzerland). *Water Resources Research*, **41**, W03006, doi:10.1029/2004WR003458 (2005).

Olivella, S., Gens, A. Vapour transport in low permeability unsaturated soils with capillary effects. *Transport In Porous Media*, **40**, 219–241 (2000).

Pousada, P.E. Deformabilidad de arcillas expansivas bajo succión controlada. *Ph. D. Thesis*, Technical University of Madrid, Spain (1982).

Rutqvist J., Barr D., Birkholzer J.T., Chijimatsu M., Kolditz O., Liu Q.-S., Oda Y, Wang W.-Q. and Zhang C.-Y. Results from an international simulation study on coupled thermal, hydrological, and mechanical (THM) processes near geological nuclear waste repositories. *Nuclear Technology*, **163**, 101–109 (2008).

Rutqvist, J., Ijiri, Y. Yamamoto, H. Implementation of the Barcelona Basic Model into TOUGH-FLAC for simulations of the geomechanical behavior of unsaturated soils. *Computers & Geosciences*, **37**, 751–762 (2011).

Rutqvist, J., Zheng, L., Chen, F., Liu, H.-H., Birkholzer, J. Modeling of coupled thermo-hydro-mechanical processes with links to geochemistry associated with bentonite-backfilled repository tunnels in clay formations. *Rock Mech. Rock Eng.*, **47**, 167–186 (2014).

Saiyouri, N., Hicher, P., Tessier, D. Microstructural approach and transfer water modeling in highly compacted unsaturated swelling clays. *Mechanics of Cohesive-Fraictional Materials*, **5**, 41–60 (2000).

Sánchez, M., Gens, A., Guimarães, L. do N., Olivella, S. A double structure generalized plasticity model for expansive materials. *Int. J. Numer. Anal. Meth. Geomech*., **29**, 751–787 (2005).

Sánchez, M., Gens, A., Guimarães, L. do N., Olivella, S. Implementation algorithm of a generalised plasticity model for swelling clays. *Computers & Geotechnics*, **35**, 860–871 (2008).

Sánchez, M., Gens, A., Olivella, S. THM analysis of a large-scale heating test incorporating material fabric changes. *Int. J. Numer. Anal. Meth. Geomech*., **36**, 391–421 (2012).

Tartakovsky, D.M. Probabilistic risk analysis in subsurface hydrology. *Geophysical Research Letters*, **34**, L05404 (2007).

Tripathy, S., Subba Rao, K.S., Fredlund, D.G. Water content – void ratio swell-shrink paths of compacted expansive soild. *Can. Geotech. J.* **39**, 938–959 (2002).

Tsang, C.F., Bernier, F., Davies, C. Geohydromechanical processes in the Excavation Damaged Zone in crystalline rock, rock salt, and indurated and plastic clays—in the context of radioactive waste disposal. *International Journal of Rock Mechanics and Mining Sciences*, **42**(1), 109-125 (2005).

Vilarrasa, V., Koyama, T., Neretnieks, I., Jing, L. Shear-induced flow channels in a single rock fracture and their effect on solute transport, *Transport In Porous Media*, **87**, 503–523 (2011).

Villar, M.V. Investigation of the behaviour of bentonite by means of suction-controlled oedometer tests. *Engineering Geology*, **54**, 67–73 (1999).

Wang, Q., Cui, Y.-J., Tang, A.M., Barnichon, J.-D., Saba, S., Ye, W.-M. Hydraulic conductivity and microstructure changes of compacted bentonite/sand mixture during hydration. *Engineering Geology*, **164**, 67–76 (2013a).

Wang, Q., Tang, A.M., Cui, Y.-J., Barnichon, J.-D., Ye, W.-M. Investigation of the hydro-mechanical behaviour of compacted bentonite/sand mixtures based on the BExM model. *Computers and Geotechnics*, **54**, 49–52 (2013b).

Yu, L., Weetjens, E., Sillen, X., Vietor, T., Li, X., Delage, P., Labiouse, V., Charlier, R. Consequences of the thermal transient on the evolution of the damaged zone around a repository for heat-emitting high-level radioactive waste in a clay formation: a performance assessment perspective. *Rock Mechanics and Rock Engineering*, **47**, 3-19 (2014).

FIGURE CAPTIONS LIST

Figure 1. Schematic representation of the two structural levels considered in the dual structure model. Clay particles are represented by the gray lines.

Figure 2. Schematic representation of the dual structure model in the isotropic plane, including the neutral line (NL) and the loading-collapse (LC) yield surface. The NL moves with the current stress state, so that the current stress state is always contained within the NL. The stress state can change along one of the following three stress paths: (i) microstructural shrinkage, if it moves to the right of the NL, (ii) microstructural swelling, if it moves to the left of the NL and (iii) neutral loading, if it moves along the NL, in which case the microstructure does not deform.

Figure 3. Evolution of (a) volumetric strain, (b) microstructural void ratio, (c) macrostructural void ratio and (d) plastic strain of the macrostructure due to micro/macrostructure interaction upon suction (wetting-drying) cycles for a net mean stress, p, of 0.01 MPa. The experimental volumetric deformation of Pousada (1982) is also displayed in (a).

Figure 4. Evolution of (a) volumetric strain, (b) microstructural void ratio, (c) macrostructural void ratio and (d) plastic strain of the macrostructure due to micro/macrostructure interaction upon suction (wetting-drying) cycles for a net mean stress, p, of 0.1 MPa. The experimental volumetric deformation of Pousada (1982) is also displayed in (a).

Figure 5. Schematic representation of the generic repository model, detail of the grid around the waste showing the monitoring points and heat power evolution for the generic repository.

Figure 6. Evolution of (a) temperature (see Figure 5 for the location of the observation points), (b) liquid saturation degree, (c) liquid pressure and (d) total mean stress for the dual structure model (DSM) and the standard single structure Barcelona Basic Model (BBM).

Figure 7. Evolution of the total and effective radial stress at point V3 located at the tunnel wall for the dual structure model (DSM) and the standard single structure Barcelona Basic Model (BBM).

Figure 8. Evolution of (a) suction, (b) net mean stress, (c) effective mean stress and (d) global bulk modulus for the dual structure model (DSM) and the standard single structure Barcelona Basic Model (BBM).

Figure 9. (a) Total porosity evolution for the dual structure model (DSM) and the standard single structure Barcelona Basic Model (BBM). (b) Macroporosity and microporosity evolution of the dual structure model.

Figure 10. Permeability evolution for the dual structure model (DSM) and the standard single structure Barcelona Basic Model (BBM). Permeability is a function of the macroporosity in the dual structure model.

Figure 11. (a) Schematic evolution of the microporosity, macroporosity, plastic strain of the macrostructure due to micro/macrostructure interaction and permeability and (b) evolution of the interaction functions for a point close to the canister (V1) and a point close to the tunnel wall (V2).

TABLES

Table 1. Parameters used to reproduce the suction cycles test of Pousada (1982).

Parameters defining the Barcelona Basic Model for macrostructural behavior						
κ_{Ps0}=0.005	κ_{sp0}=0.01	λ_{Ps0}=0.024	p^c(MPa)=0.01	r=0.85	ξ(MPa^{-1})=0.2	p_0^*(MPa)=0.75

Parameters defining the law for microstructural behavior

α_m (MPa^{-1})=1.2 β_m (MPa^{-1})=0.02

Interaction functions between the microstructure and the macrostructure

$f_c = 1.975 + 0.185 \tanh\left[5\left(p/p_0 - 0.275\right)\right]$ $f_s = 1.825 - 0.4 \tanh\left[-0.4\left(p/p_0 - 0.3\right)\right]$

e_{micro}=0.45 e_{macro}=0.55

Table 2. Properties of the clay host rock (Gens et al., 2007; Corkum and Martin, 2007).

Property	Value
Porosity, φ (-)	0.15

Young's modulus, E (GPa)	5
Poisson ratio, ν (-)	0.3
Grain density, ρ_s (kg/m^3)	2400
Grain Specific heat, C_s (J/kg/ºC)	900
Thermal conductivity, λ_T (W/m/K)	2.2
Thermal expansion coefficient, α_0 (ºC^{-1})	1.0x10^{-5}
Intrinsic permeability, k (m^2)	5.0x10^{-20}
van Genuchten water retention parameter m (-)	0.41
van Genuchten entry pressure, P_0 (MPa)	48
Residual liquid saturation, S_{lr} (-)	0.1
Residual gas saturation, S_{gr} (-)	0.01

Table 3. Material parameter values for the bentonite buffer used in the BBM model (Gens et al., 2009).

Property	Value
Initial dry density, ρ_d (kg/m^3)	1600
Compressibility parameter for stress-induced elastic strain, κ_{Ps0} (-)	0.05
Compressibility parameter for suction-induced elastic strain, κ_{sp0} (-)	0.25
Poisson ratio, ν (-)	0.4
Parameter for stress-induced elastic strain, α_{ps} (MPa^{-1})	-0.003
Parameter for suction-induced elastic strain, α_{sp} (-)	-0.161
Parameter for suction-induced elastic strain, α_{ss} (-)	0
Reference stress state for relating elastic compressibility to suction, p_{ref} (MPa)	0.01
Thermal expansion coefficient, α_0 (ºC^{-1})	1.5x10^{-5}
Compressibility parameter in virgin state soils at zero suction, λ_{Ps0} (-)	0.15
Parameter defining soil stiffness associated with loading collapse yield, r (-)	0.925
Parameter for the increase of soil stiffness with suction, ξ (MPa^{-1})	0.1
Parameter that describes the increase of cohesion with suction, k_s (-)	0.1
A reference stress state for compressibility relation in virgin states, p^c (MPa)	0.5
Slope of the critical state line, M (-)	1.0

Non-associativity parameter in the plasticity flow rule, α_a (-)	0.53
Specific volume at reference stress state p^c in virgin state, v^c (-)	1.937
Net mean yield stress for saturated conditions at reference temperature, p_0^* (MPa)	12.0
Initial porosity, φ_0 (-)	0.398
Saturated reference permeability at reference porosity φ_0, k_0 (m^2)	4.5x10^{-27}
Reference porosity for the permeability model, φ_0 (-)	0.14
Model parameter for permeability, b (-)	50
Relative permeability to liquid, k_{rl} (-)	$k_{rl} = S_l^3$
Relative permeability to gas, k_{rg} (-)	$k_{rg} = 1$
Klinkenberg parameter, b_k (MPa)	2.5x10^5
van Genuchten water retention parameter m (-)	0.32
van Genuchten entry pressure, P_0 (MPa)	30
Residual liquid saturation, S_{lr} (-)	0.1
Residual gas saturation, S_{gr} (-)	0
Grain Specific heat, C_s (J/kg/ºC)	800
Thermal conductivity, λ_T (W/m/K)	$0.5 + S_l(1.3 - 0.5)$

Table 4. Material parameter values of the bentonite buffer used in the dual structure model (only the parameters of the macrostructure that differ from those used for the BBM model (Table 3) are included here) (Sanchez et al., 2012).

Property	Value
Compressibility parameter for stress-induced elastic strain, κ_{Ps0} (-)	0.079
Compressibility parameter for suction-induced elastic strain, κ_{sp0} (-)	0.08
Reference stress state for relating elastic compressibility to suction, p_{ref} (MPa)	0.03
Specific volume at reference stress state p^c in virgin state, v^c (-)	1.4935
Initial void ratio of the macrostructure, e_M (-)	0.35
Initial void ratio of the microstructure, e_m (-)	0.3
Parameter controlling the microstructural soil stiffness, α_m (MPa^{-1})	0.006

Parameter controlling the microstructural soil stiffness, β_m (MPa^{-1})	0.0027
Interaction function for microstructural swelling paths	$f_s = 0.8 - 1.1\tanh\left[20\left(p/p_0 - 0.25\right)\right]$
Interaction function for microstructural compression paths	$f_c = 1.0 + 0.9\tanh\left[20\left(p/p_0 - 0.25\right)\right]$
Saturated reference permeability at reference porosity φ_0, k_0 (m^2)	3.0x10^{-23}
Reference porosity of the macrostructure for the permeability model, φ_{M0} (-)	0.14

FIGURES

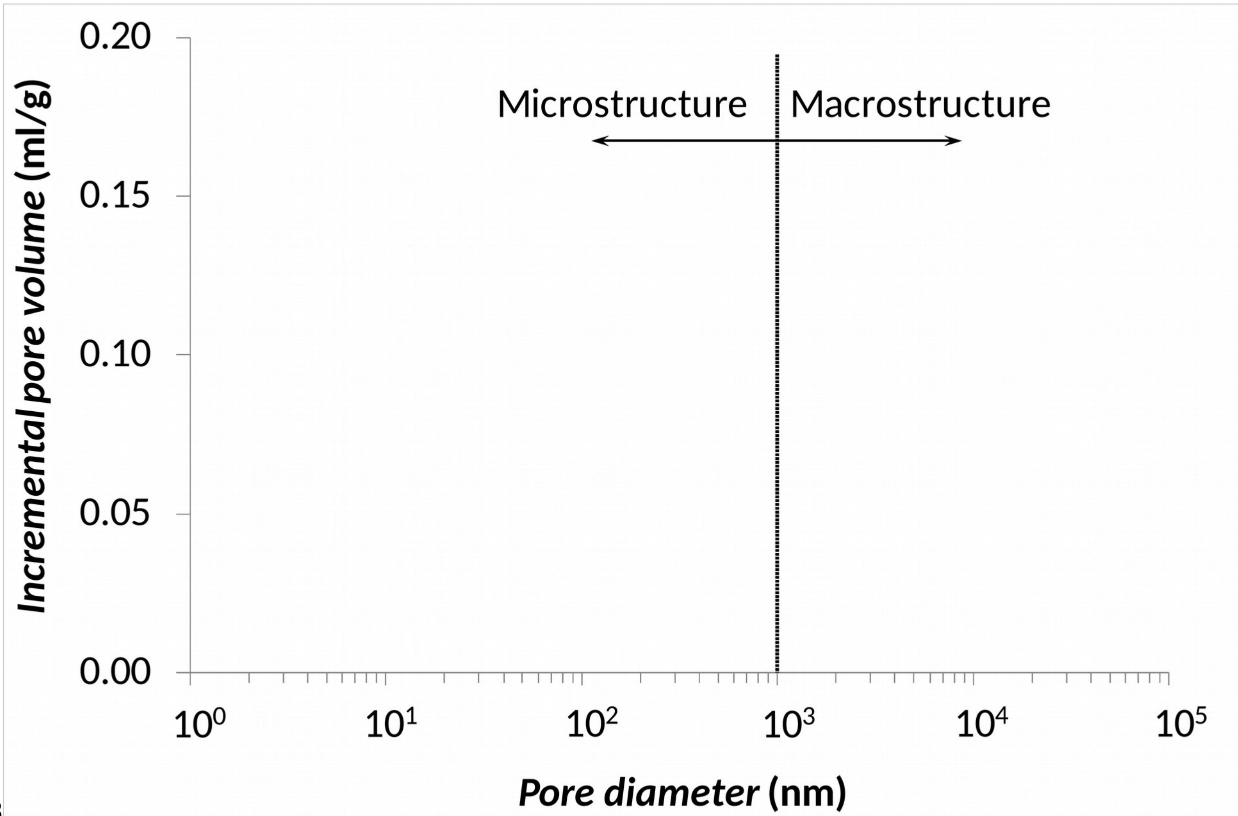

Figure 1. Bimodal pore size distribution of an expansive soil measured from mercury intrusion porosimetry (adapted from Lloret et al., 2003).

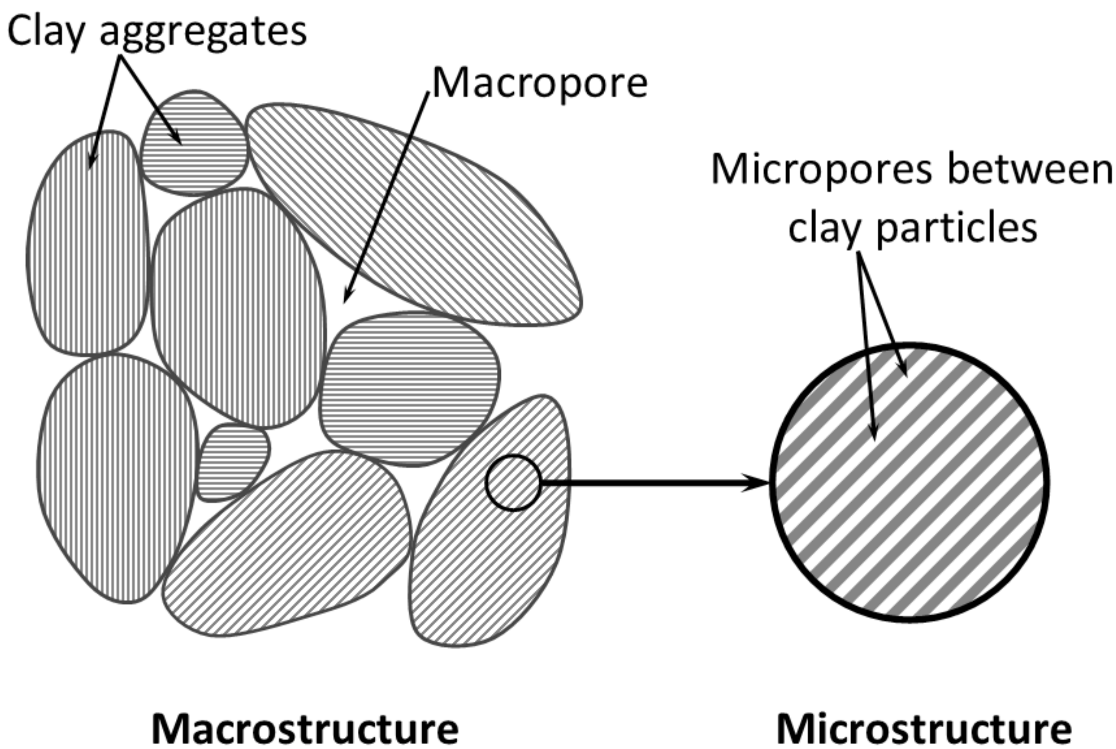

Figure 2. Schematic representation of the two structural levels considered in the dual structure model. Clay particles are represented by the gray lines.

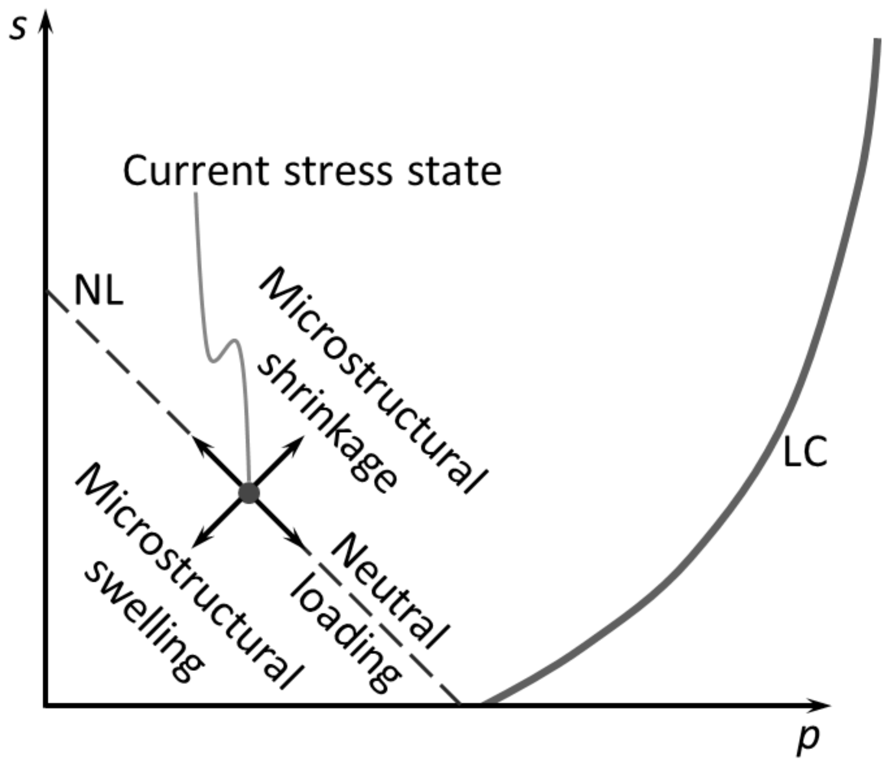

Figure 3. Schematic representation of the dual structure model in the isotropic plane, including the neutral line (NL) and the loading-collapse (LC) yield surface. The NL moves with the current stress state, so that the current stress state is always contained within the NL. The stress state can change along one of the following three stress paths: (i) microstructural shrinkage, if it moves to the right of the NL, (ii) microstructural swelling, if it moves to the left of the NL and (iii) neutral loading, if it moves along the NL, in which case the microstructure does not deform.

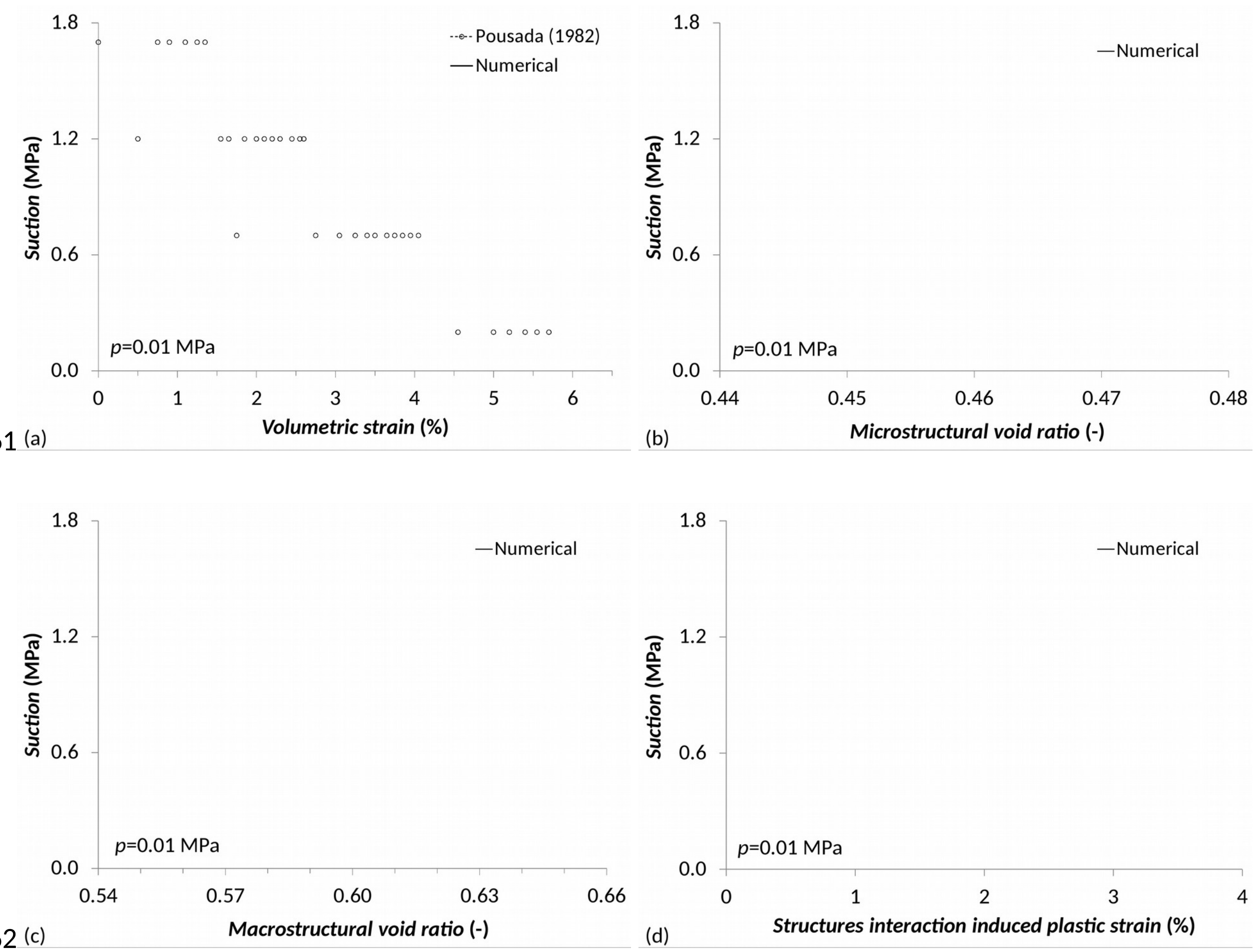

Figure 4. Evolution of (a) volumetric strain, (b) microstructural void ratio, (c) macrostructural void ratio and (d) plastic strain of the macrostructure due to micro/macrostructure interaction upon suction (wetting-drying) cycles for a net mean stress, p, of 0.01 MPa. The experimental volumetric deformation of Pousada (1982) is also displayed in (a).

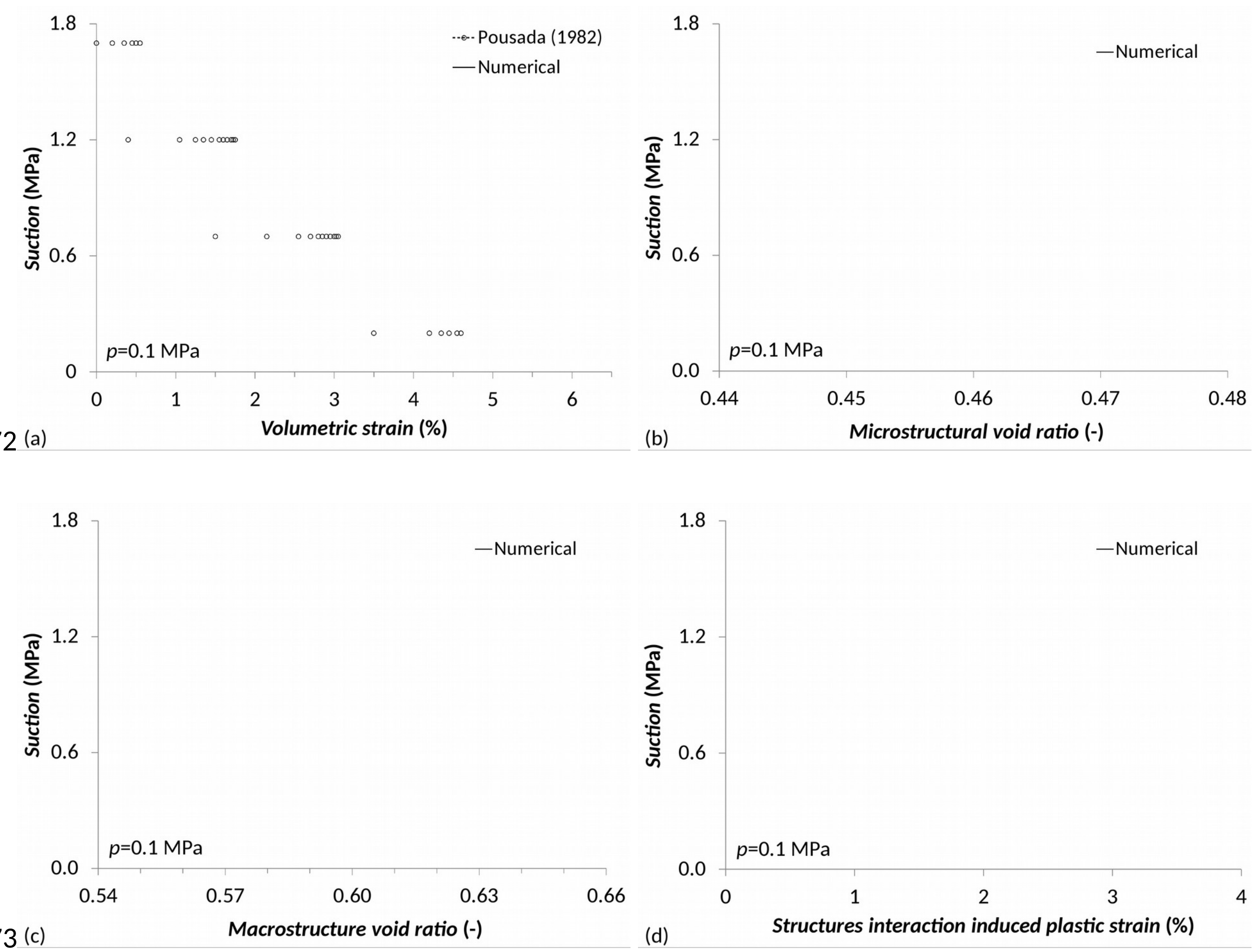

Figure 5. Evolution of (a) volumetric strain, (b) microstructural void ratio, (c) macrostructural void ratio and (d) plastic strain of the macrostructure due to micro/macrostructure interaction upon suction (wetting-drying) cycles for a net mean stress, p, of 0.1 MPa. The experimental volumetric deformation of Pousada (1982) is also displayed in (a).

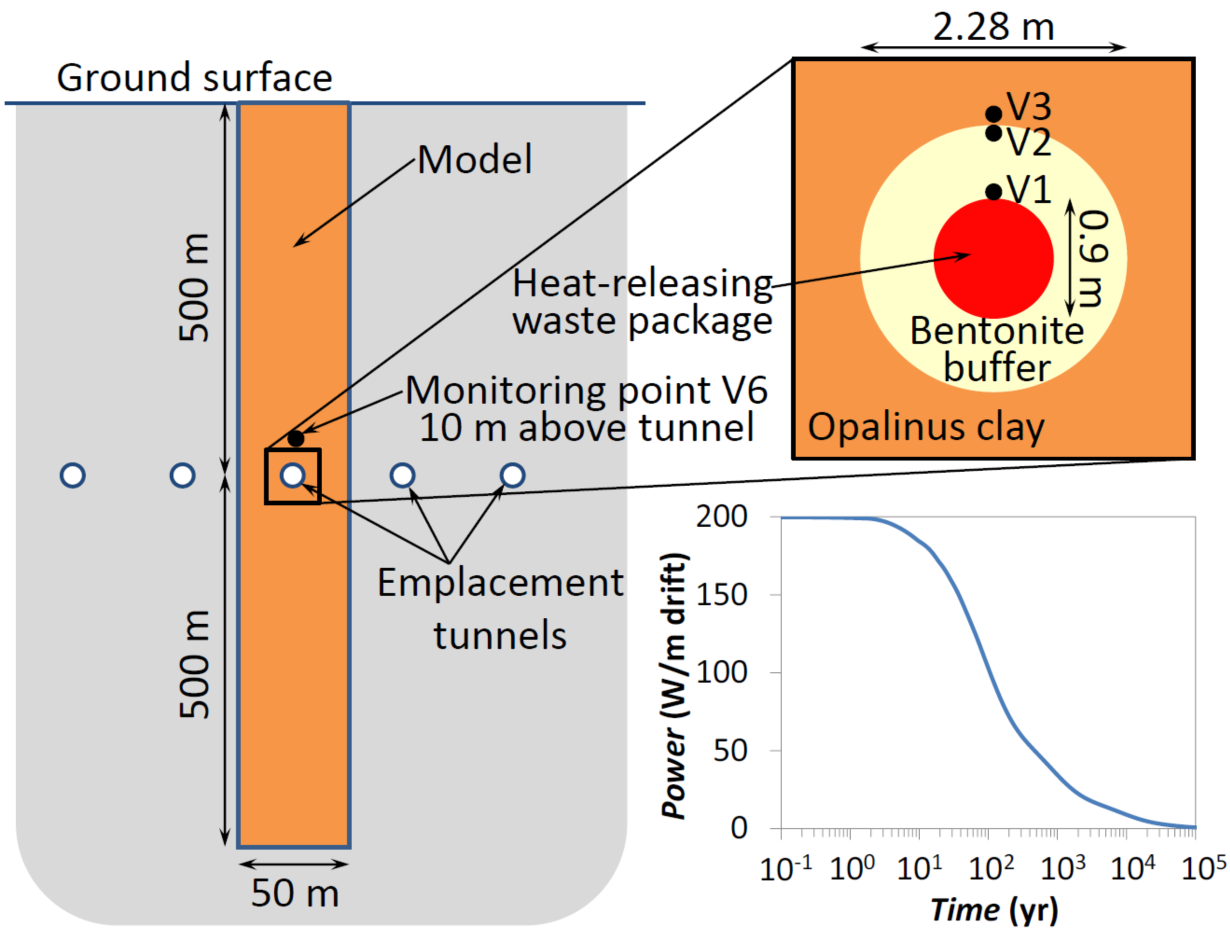

Figure 6. Schematic representation of the generic repository model, detail of the grid around the waste showing the monitoring points and heat power evolution for the generic repository.

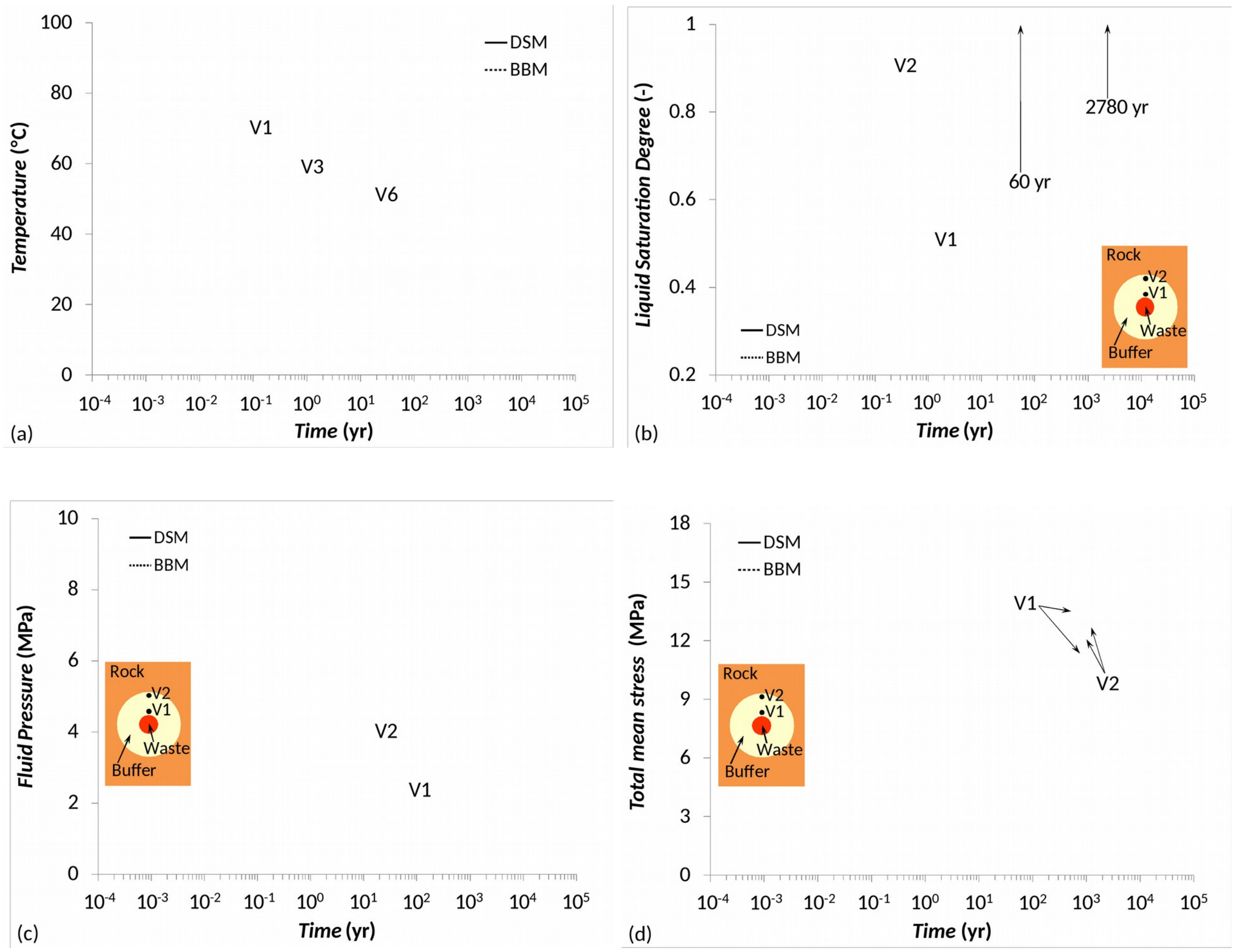

Figure 7. Evolution of (a) temperature (see Figure 5 for the location of the observation points), (b) liquid saturation degree, (c) liquid pressure and (d) total mean stress for the dual structure model (DSM) and the standard single structure Barcelona Basic Model (BBM).

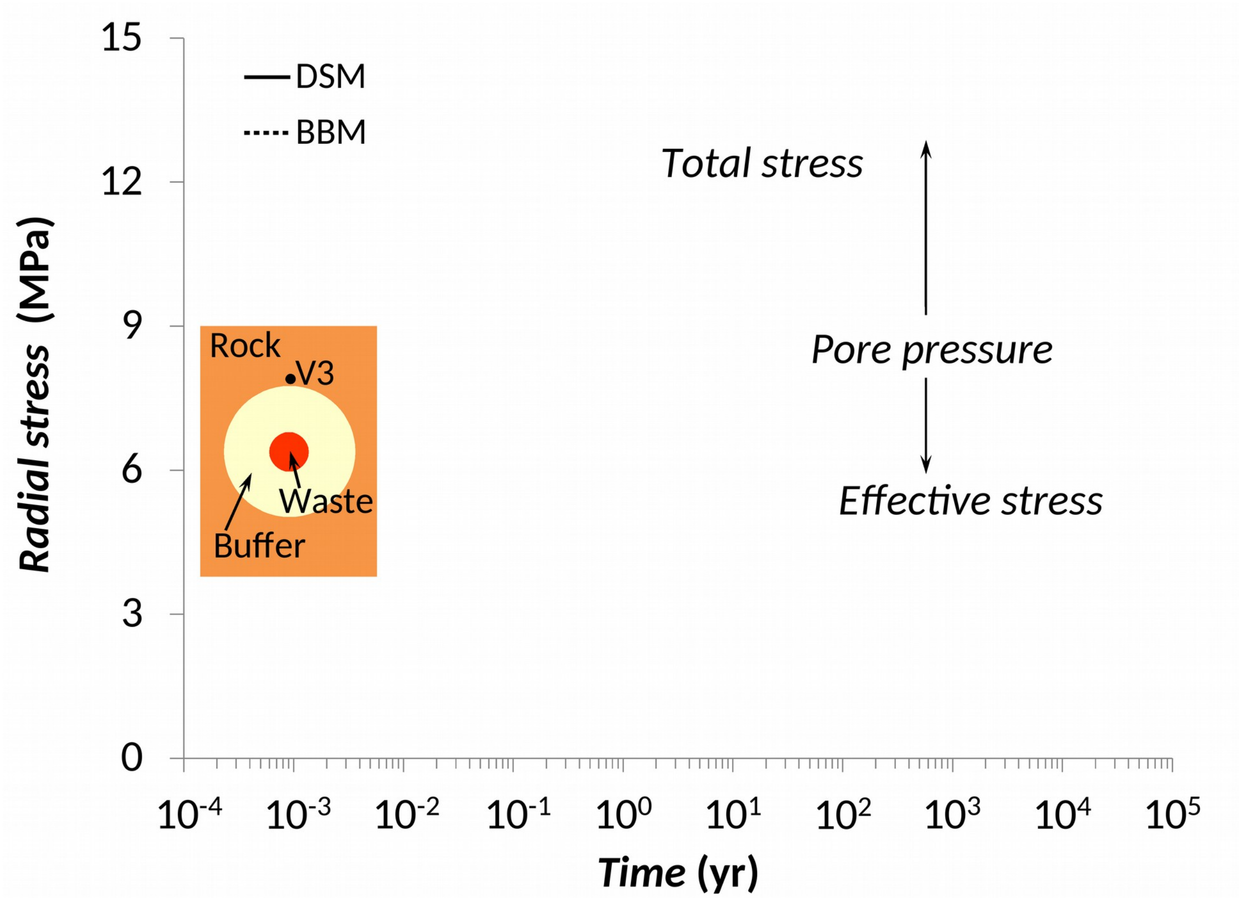

Figure 8. Evolution of the total and effective radial stress at point V3 located at the tunnel wall for the dual structure model (DSM) and the standard single structure Barcelona Basic Model (BBM).

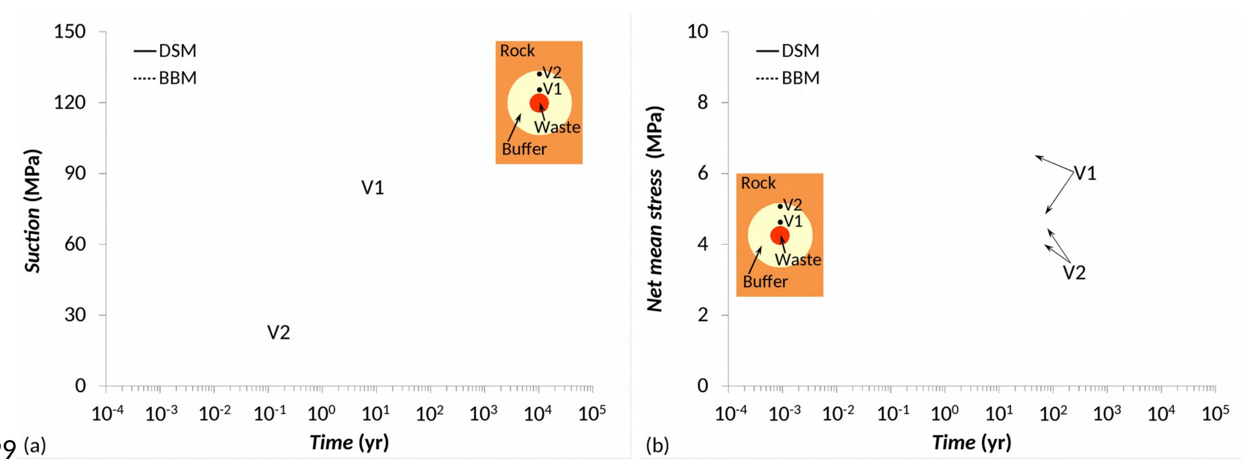

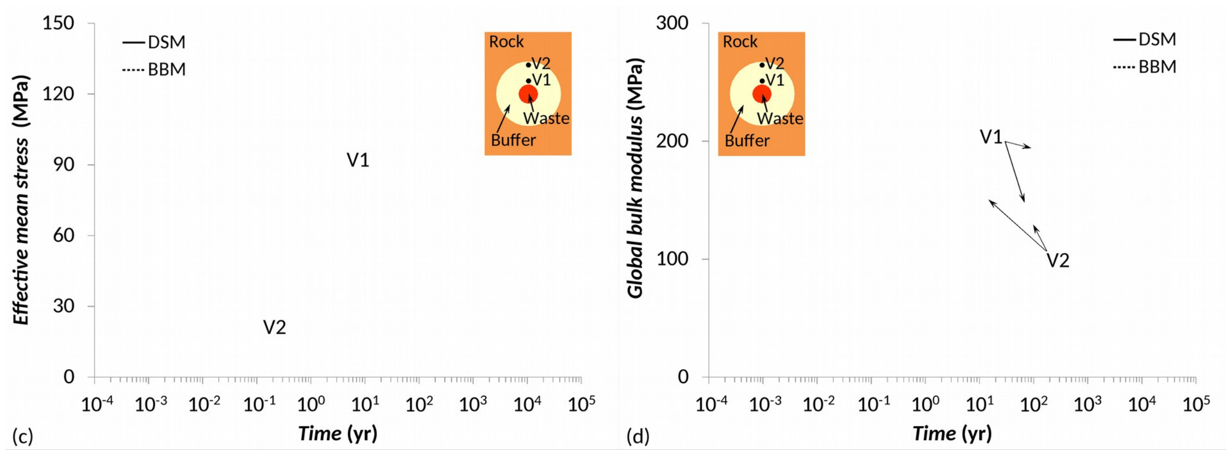

Figure 9. Evolution of (a) suction, (b) net mean stress, (c) effective mean stress and (d) global bulk modulus for the dual structure model (DSM) and the standard single structure Barcelona Basic Model (BBM).

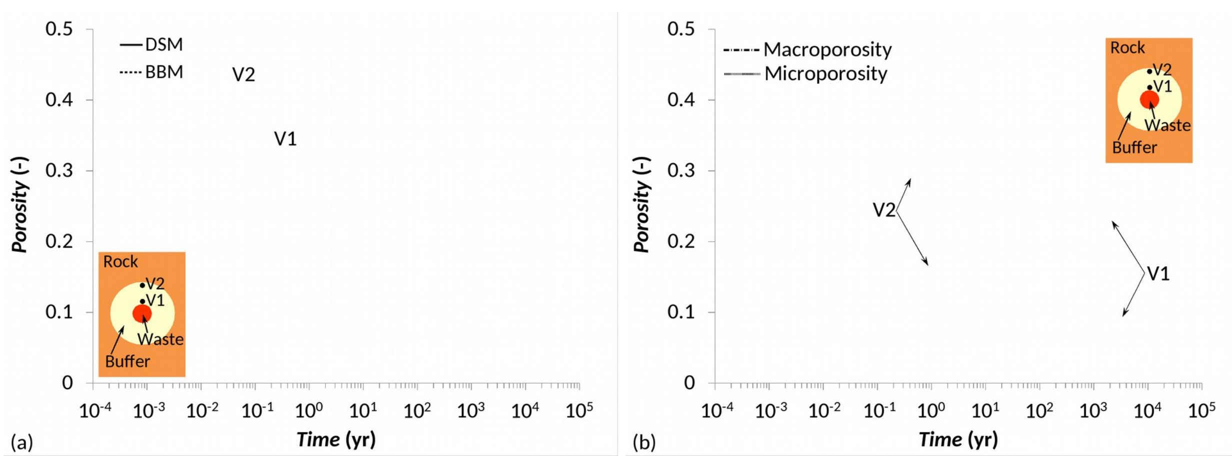

Figure 10. (a) Total porosity evolution for the dual structure model (DSM) and the standard single structure Barcelona Basic Model (BBM). (b) Macroporosity and microporosity evolution of the dual structure model.

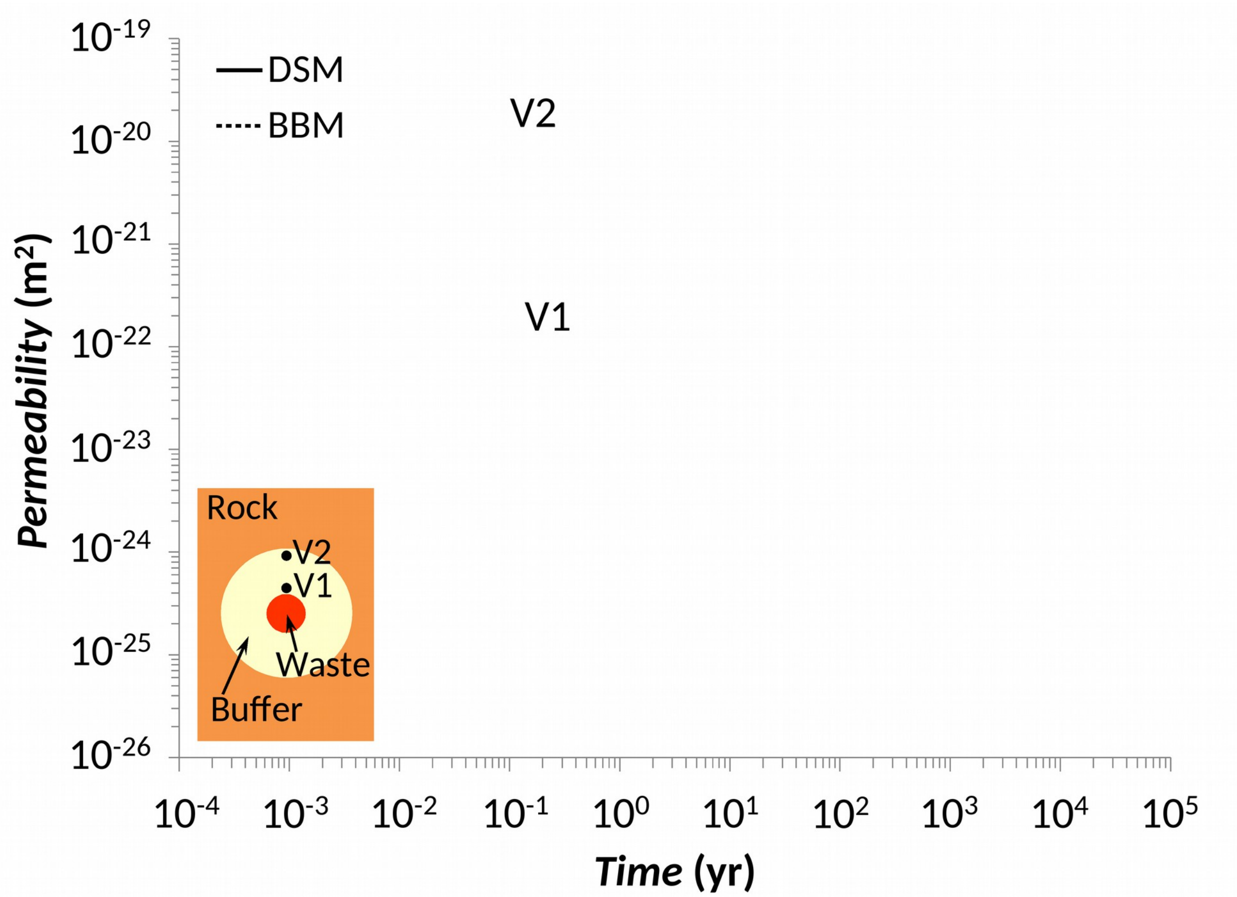

Figure 11. Permeability evolution for the dual structure model (DSM) and the standard single structure Barcelona Basic Model (BBM). Permeability is a function of the macroporosity in the dual structure model.

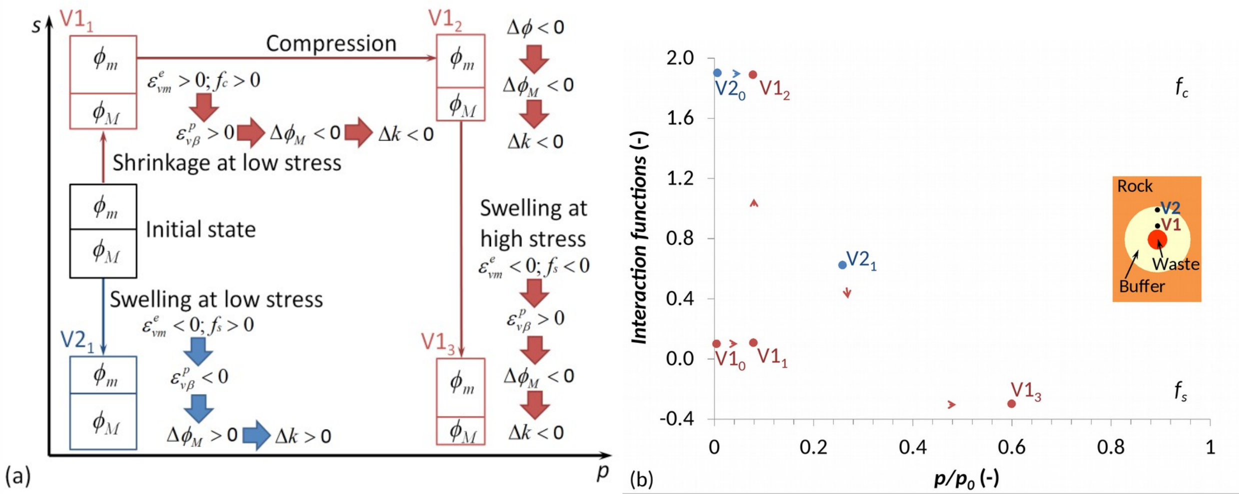

Figure 12. (a) Schematic evolution of the microporosity, macroporosity, plastic strain of the macrostructure due to micro/macrostructure interaction and permeability and (b) evolution of the interaction functions for a point close to the canister (V1) and a point close to the tunnel wall (V2). Note that the sign criterion of geomechanics is adopted, i.e., strain is positive in compression and negative in extension.